Available online at www.eccomasproceedia.org
Eccomas Proceedia COMPDYN (2023) 1104-1115

ECCOMAS
Proceedia

COMPDYN 2023
9th ECCOMAS Thematic Conference on
Computational Methods in Structural Dynamics and Earthquake Engineering
M. Papadrakakis, M. Fragiadakis (eds.)
Athens, Greece, 12-14 June 2023

FRAGILITY CURVES ASSESSMENT OF AN EXISTING TYPOLOGICAL RC BUILDING SUBJECTED TO THE COMBINED ACTION OF SLOW-MOVING SETTLEMENTS AND EARTHQUAKE

Andrea Miano[1], Annalisa Mele[1], Carlo Del Gaudio[1], Gerardo Mario Verderame[1], and Andrea Prota[1]

[1] Department of Structures for Engineering and Architecture, University of Naples "Federico II"

Via Claudio 21, 80125 Naples, Italy

{andrea.miano, annalisa.mele, carlo.delgaudio, verderam, aprota}@unina.it

Abstract

The seismic assessment of reinforced concrete (RC) structures is commonly carried out neglecting potential previous damage induced by other phenomena, for example those related to the actions of slow-moving settlements. Many efforts are dedicated by the research community in properly considering multi-hazard actions and their inter-relations on the structure, instead of a reductionist approach, to be included in the numerical models adopted for the assessment of the seismic vulnerability. Such a consequences are increasingly becoming an important issue in the structural assessment, since several structures have an age close to, or higher than their design life. In this work a typological 3D case study RC building, including also infills, is created according to gravity loads design. The seismic assessment of the building structural elements, caused by the design seismic action, is initially shown. Then, the seismic assessment is repeated, considering as point zero of the analysis the "damaged" building as consequence of known slow-moving settlements. Finally, an interesting comparison in terms of fragility curves is proposed between the safety condition of the building expected in both cases, with or without the consideration of the precedent induced displacements.

Keywords: Fragility curves, Combined Risk, Multi-Hazard Assessment, Existing RC Buildings, Remote sensing.

ISSN:2623-3347
Peer-review under responsibility of the organizing committee of COMPDYN 2023.
doi: 10.7712/120123.10461.21278

1 INTRODUCTION

The seismic assessment of reinforced concrete (RC) structures is commonly carried out neglecting potential previous damage induced by other phenomena, for example those related to the actions of slow-moving settlements. In general, different forms of hazard can affect structures throughout their existence, generally not occurring simultaneously, but spaced over the years. This is a scenario that may very likely occur, for example, in Italy, that is one of the countries worldwide most affected by landslides, also known for being a territory characterized by high seismicity. Many efforts are dedicated by the research community in properly considering multi-hazard actions and their inter-relations on the structure, instead of a reductionist approach, to be included in the numerical models adopted for the assessment of the seismic vulnerability. Such a consequences are increasingly becoming an important issue in the structural assessment, since several structures have an age close to, or higher than their design life. The previous damage that can affect the RC structures at the moment of the seismic assessment can be related to different hazards. At this regard, there are some applications that evaluates the structural damage in existing RC structures as consequence of displacements induced by different hazards, such as landslides [1,2] and subsidence [3-5]. Instead, the research on the seismic assessment procedures for existing RC buildings affected by slow-moving landslides or different hazard sources-induced displacements is very limited. Fotopoulou et al., 2015 [6] assessed the vulnerability of RC buildings subjected to seismically induced slope displacements with an analytical approach. Instead, Negulescu et al., 2010 [7]. proposed fragility curves for masonry structures subjected to permanent ground displacements and earthquakes. Then, Miano et al., 2022 [8] proposed fragility curves for different classes of existing RC buildings under ground differential settlements. Finally, Mele et al. [9] studied the combined risk landslide-earthquake for a case study building.

With respect to the seismic fragility curves evaluation, it is possible to make a distinction based on the type of data used for deriving them, into four categories [10]; namely, analytic (e.g., [8,11]), empirical (e.g., [12-14]), based on expert opinion, and hybrid (e.g., [15]). In this work, a specific focus is done on the analytical approach in order to study the effect of the previous damage condition on the fragility estimation.

In particular, a typological 3D case study RC building, including also infills, is created according to gravity loads design. The seismic assessment of the building structural elements, caused by the design seismic action, is initially shown. Then, the seismic assessment is repeated, considering as point zero of the analysis the “damaged” building as consequence of known slow-moving settlements. The non linear dynamic analysis known as Cloud is implemented herein on the equivalent SDOF system coming from the pushover analysis. Finally, an interesting comparison in terms of fragility curves is proposed between the safety condition of the building expected in both cases, with or without the consideration of the precedent induced displacements.

2 METHODOLOGY

2.1 Fragility analysis framework

The first point of the methodology is to derive the equivalent SDOF and to mark the damage states on the pushover curve. Consider the equivalent SDOF system that is derived based on the static pushover analysis on the MDOF structure, given the assigned load patterns (see [16,17]). The damage states are defined at the MDOF level as reported in Section 2.2.

In this study the onset of a given damage state is quantified by employing a system-level damage measure defined for a prescribed damage state as the critical demand to capacity ratio (DCR_{LS}) for the component that takes the structure closest to the onset of the damage state [19]. In other words, DCR_{LS} is expressed in a fully deformation-based manner as the maximum of DCR_{LS} values for all the structural elements expressed as the ratio of chord rotation/displacement demand to chord rotation/displacement capacity for that damage state. The concept of demand to capacity ratio can also be extended to the equivalent EPP system at the SDOF level in a straight-forward manner as the ratio of the displacement demand for the equivalent SDOF system and the displacement at the onset of damage state that is mapped to the SDOF level.

With regards to seismic assessment and retrofit fragility analysis, Cloud Analysis is used [18-20]. Cloud Analysis is employed herein for the equivalent single-degree-of-freedom EPP system [21]. Once the ground motion records are applied to the structure, the critical demand over capacity ratio for the selected limit state (DCR_{LS}) is found. This provides a set of values that form the basis for the cloud-method calculations. The statistical properties of the cloud response are calculated through a logarithmic linear regression applied to the response. This is equivalent to fitting a power-law curve to the cloud response in the original (arithmetic) scale. This results in a curve that finds the median drift demand for a given level of acceleration:

$$\begin{aligned} &\eta_{DCR|Sa}(Sa) = a \cdot Sa^b \\ &\ln(\eta_{DCR|Sa}(Sa)) = \ln(a) + b \cdot \ln(Sa) \end{aligned} \tag{1}$$

where ln(a) and b are regression constants. The logarithmic standard deviation $\beta_{DCR|Sa}$ is the root mean sum of the square of the residuals with respect to the regression prediction:

$$\beta_{DCR|Sa} = \sqrt{\frac{\sum(\ln(DCR_i) - \ln(a \cdot S_{a,i}{}^b))^2}{N-2}} \tag{2}$$

where DCR_i and $Sa_{,i}$ are the demand over capacity ratio values and the corresponding S_a for record number i within the cloud response set and N is total number of records. The standard deviation of regression, as introduced in the preceding equation, is presumed to be constant with respect to S_a over the range of S_a in the cloud. Finally, the structural fragility curves based on the Cloud Analysis can be expressed as:

$$\begin{aligned} &P\left(DCR > 1 \middle| S_a\right) = P(\ln DCR > 0 \middle| S_a) = \\ &1 - \Phi\left(\frac{-\ln \eta_{DCR|S_a}}{\beta_{DCR|S_a}}\right) = \Phi\left(\frac{\ln \eta_{DCR|S_a}}{\beta_{DCR|S_a}}\right) \end{aligned} \tag{3}$$

2.2 Damage states definition

The definition of global Damage States, DS, adopted in present study is pursuant to classification proposed by the European Macroseismic Scale (Grunthal, 1998 [22]) at building level, where an in-depth qualitative and quantitative representation of damage suffered by the different components is reported by increasing its severity. Given the mechanical basis of the procedure, this representation is herein referred to engineering demand parameters (i.e., interstorey drift ratio, axial displacement) properly chosen to characterize the onset of damage patterns depicted by EMS-98 damage classification on single component.

This association is made taking advantage of the phenomenological analysis present in the literature (Cardone and Perrone, 2015 [23]; Del Gaudio et al., 2019 [24]), where the authors quantify the thresholds and its uncertainties corresponding to given EMS-98 damage stated,

by means of a throughout analysis of all the experimental campaign texts available at that time. This is the case of damage classification made for infill panels, where the axial displacement capacity is set with reference to its response curve, i.e. set coinciding with predetermined percentages (0.3 for DS1, 1.0 for DS2, 2.5 for DS3 according to Cardone and Perrone, 2015 [23]) of the displacement where the infill attains the peak resistance. The thresholds assumed herein for infill panels result also in good agreement with those statistically obtained in (Del Gaudio et al., 2019 [24]) by analyzing over than 200 experimental texts on infilled reinforced concrete frames. It has to be noted that according to EMS classification, the failure of individual infill panels is achieved for a DS3, thereafter damage analysis is controlled by the structural elements. Moreover, damage states analysis for structural elements (columns and beams) is considered herein only with reference to flexural behaviour.

Thus, the IDR capacity for RC columns expected to fail in flexure is established according to the assumptions reported in (Del Gaudio et al., 2017 [25] and Del Gaudio et al., 2018 [26]): **DS1** (*Fine cracks in plaster over frame members*) can be set at the onset of the first visible cracks; in other words, it can be referred to the first attainment of the cracking moment at the element end section. **DS2** (*Cracks in columns and beams of frames*) can be associated with the widening of flexural cracks that occurs when longitudinal reinforcement yields, thus to the first attainment of the yielding moment element. **DS3** (*Cracks in columns and beam column joints of frames at the base and at joints of coupled walls. Spalling of concrete cover, buckling of reinforced rods.*) can be associated with the attainment of peak strength in nonlinear response curve of the element. **DS4** (*Large cracks in structural elements with compression failure of concrete and fracture of rebars; bond failure of beam reinforced bars*) can be assumed to correspond to the first stage of post-peak degrading branch of nonlinear response curve of elements, or in other words to that displacement where response losses 20% of its peak strength. **DS5** (*Collapse of ground floor or parts of buildings*) is set at the attainment of the IDR corresponding to the zero resistance point of the backbone curve of element.

In order to potentially consider the flexural-shear interaction in the response, a preclassification, to determine their expected failure mode through the comparison between the flexural plastic shear and the shear strength, can be implemented. Hence, each element can be classified as flexure, shear or flexure-shear as a function of the ratio between flexural shear and shear strength. In this case, the IDR capacity for RC columns expected to fail in shear or flexure-shear differs from the flexure type only for most severe damage states: DS4 can be set at the onset of Shear failure displacement according to the study by Aslani and Miranda, 2005 [27]. Then, also DS5 can be set at the onset of the loss of vertical load carrying capacity (Axial Failure), which is also provided by Aslani and Miranda, 2005 [27].

3 APPLICATION

3.1 Case study building

The building considered in this study shares the same typical architectural layout already used for code-conforming buildings in Di Domenico et al., 2022 [28] and De Risi et al., 2022 [29]. The considered Prototype Building is supposed to been designed in 1970s, constituted by 3 storeys with a rectangular plan, which global dimensions are equal to 20.80 m and 11.80 m, respectively. The plan layout consists of a grid of five spans along the longitudinal axis X and three spans along the transverse axis Y, where X and Y are the directions parallel to the two orthogonal layout of walls of the structure. A top view of the structural model, that will be described in Section 3.2, is shown in Figure 1.

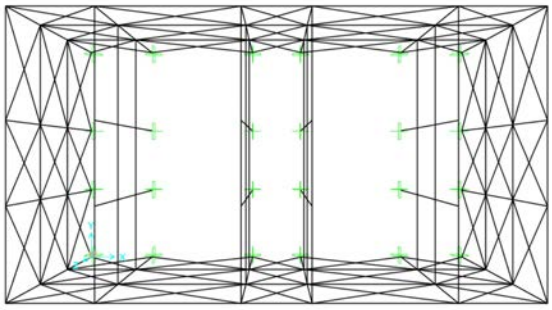

Figure 1: Top view of the structural model.

The building structural characteristics are obtained following a simulated design procedure based on design code prescriptions, professional practices and seismic classification of the area of interest at the time of construction, according to (Verderame et al., 2010 [30]). Dead loads are evaluated from a load analysis, whereas live loads are evaluated from past code prescriptions for ordinary structures. Element dimensions are calculated according to the allowable stresses method; the design value for maximum concrete compressive stress is assumed equal to 5.0 and 7.5 MPa for axial load and axial load combined with bending respectively. Column dimensions are calculated according only to the axial load, beam dimensions are determined from bending due to loads from slabs. Column reinforcement is designed according to minimum longitudinal reinforcement geometric ratio prescribed by code for gravity load designed buildings.

3.2 Modeling approach

A finite element model (FEM) structural model of the building has been created (Figure 1), where beams and columns have been modelled as mono-dimensional elements, as well as the infills, for which an equivalent strut model has been considered according to Al-Chaar, 2002 [31] and Fardis, 2009 [32]. The columns at the base have been assumed to be fixed.

A concentrated plasticity model has been considered for the RC elements (see Figure 2a,b), considering the non-linear flexural behavior at the ends. In particular, the non-linear behavior of each RC column is characterized by a tri-linear envelope, with cracking and yielding as characteristic points. Behavior is linear elastic up to cracking and perfectly-plastic after yielding. Moment at yielding (M_y) is calculated in closed form by means of the first principles-based simplified formulations proposed in Biskinis and Fardis, 2010 a-b [33,34].

Lateral force–displacement relationships for infill panels are evaluated according to the model proposed by Panagiotakos and Fardis, 1996 [35] (see Figure 2c) and applied in the middle of the equivalent strut.

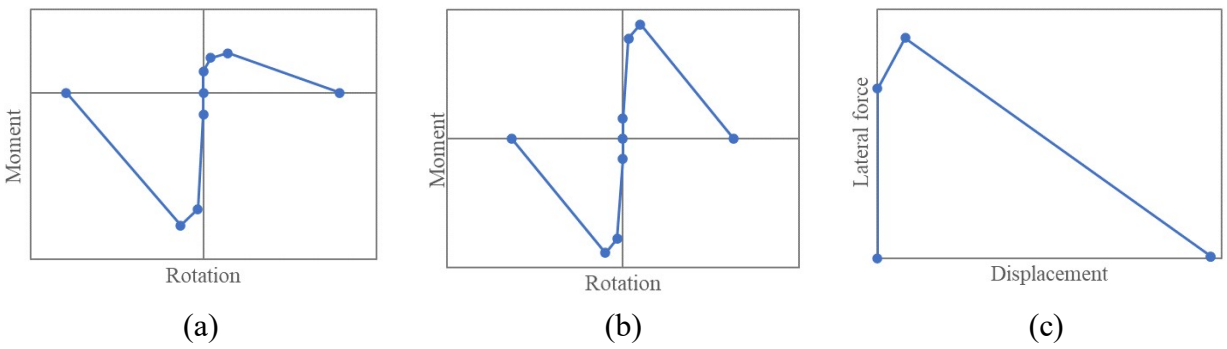

Figure 2: Schematization of the non-linear behavior of (a) columns, (b) beams, and (c) infills.

3.3 Results

In this work, a pattern of differential vertical settlements has been imposed at the base of the columns in the structural model to analyze their effects on the RC building' response, to seismic action.

It is supposed the existence of a deformation pattern increasing from one side of the building to the opposite one, along its Y side (see Figure 1). This deformation condition can represent, for example, a subsidence phenomenon [5]. However, the identification of the causes of the displacements is not a goal of this work.

In the first year, the settlements at the two end columns are ρ_{min} and ρ_{max}, equal to 1 mm and 4 mm respectively, for a differential settlement $\Delta\rho$ of 3 mm. It is hypothesized an increase of 1 mm per year, for a total period of 50 years. The 50 settlement profiles are illustrated in Figure 3.

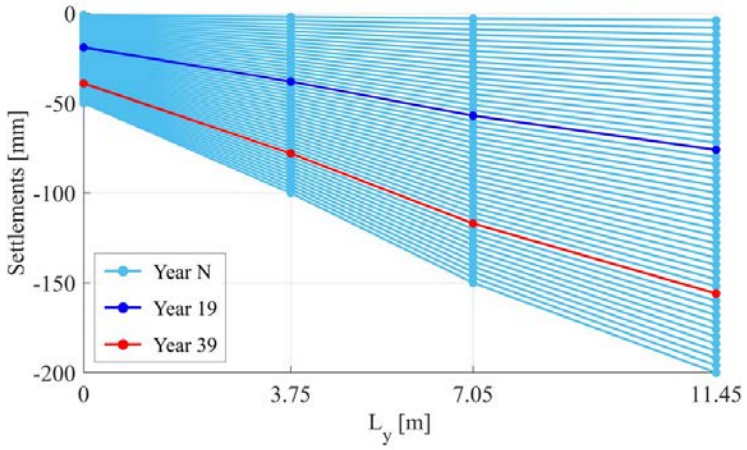

Figure 3: Displacement patterns applied in Y direction for N years (where N ranges between 1 and 50).

Initially, pushover analyses in the two directions parallel to the building sides are carried out according to the Italian code ([17], [36]), by subjecting the structure to a monotonically increasing pattern of lateral forces, starting from the gravity-loads-deformed structure. The pushover analysis that gives the most significative demand on the structure is those with the distribution of forces proportional to the masses, in the Y direction (MassY+). For brevity, only the results of this analysis will be shown in the following. The pushover analysis results for the case of seismic action applied on the gravity loads deformed structure are shown in Figure 4, where the pushover curve referred to the multi-degree of freedom (MDOF) model (continuous black line), the capacity curve referred to the equivalent single-degree of freedom (SDOF) (black dashed line), and the equivalent bilinear curve referred to the SDOF (dash-dot gray line) are represented. The capacity curve of the equivalent SDOF system is obtained by dividing the pushover curve by the modal participation factor Γ. The bilinearization of the capacity curve is carried out as indicated in the Italian code ([17], [36]).

The d*-F* couples corresponding to the reaching of the five DS are represented with colored circular markers (green for DS1, yellow for DS2, red for DS3, blue fort D4, and magenta for DS5). At every year, a non-linear incremental analysis has been implemented, considering the earthquake action applied to the model, starting from its configuration deformed as a consequence of the applied settlements. The analyses are repeated for 50 years, with the base displacements' amplitude scaled up as previously described.

For each analysis, the structural assessments for the RC elements and the infills have been conducted, and the increase in demand has been analysed according to the DSs described in

Section 2.2, to understand which displacement profile induced for the first time a particular DS for at least one element of the structure.

The settlement configurations inducing for the first time the DS1 and the DS2 are represented in Figure 3 with a blue and a red line, respectively. For brevity, the pushover analysis results are shown only for these two analyses, in Figure 4b and Figure 4c, for DS1 and DS2, respectively. In particular, DS1 is attained at the 19th year, that means ρ_{min} and ρ_{max}, equal to 19 mm and 76 mm respectively, for a differential settlement $\Delta\rho$ of 57 mm. DS2, instead, is attained at the 39th year, that means ρ_{min} and ρ_{max}, equal to 39 mm and 156 mm respectively, for a differential settlement $\Delta\rho$ of 177 mm. The subsidence action induces stresses and strains in the structural elements, so the seismic action is applied on an already solicited model.

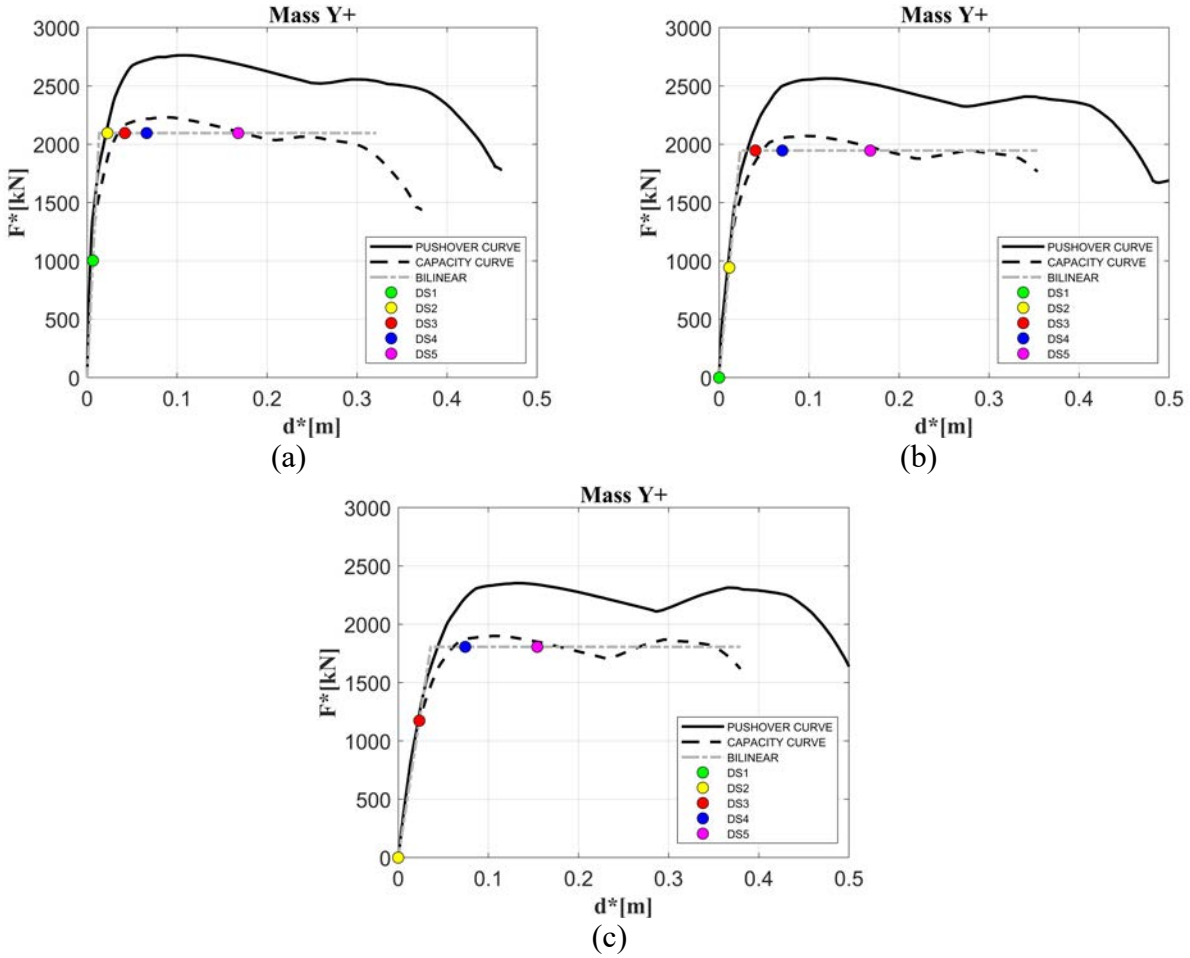

Figure 4: Pushover curves for cases (a) Mass Y+ case, (b) Mass Y+ at year 19 (c) Mass Y+ at year 39.

As mentioned in the methodological section, Cloud Analysis, which consists of a series of non-linear time history analyses considering a large database of unscaled ground-motion records, is then applied. For this application, the SIMBAD database (Selected Input Motions for displacement-Based Assessment and Design, Smerzini et al., 2014 [37]) is adopted. SIMBAD includes 467 tri-axial accelerograms, generated by 130 worldwide seismic events (shallow crustal earthquakes with magnitudes from 5 to 7.3 and epicentral distances up to 35 km). As in Rossetto et al., 2016 [38] and Gentile et al., 2019 [39], a subset of 150 records is considered by first ranking the 467 records in terms of their PGA values (by using the geometric mean of the two horizontal components) and then keeping the component with the largest PGA value (for the 150 stations with highest mean PGA).

Figure 5(a,b,c) demonstrate the results of the Cloud Analysis for the five damage states in the logarithmic scale. The set of 150 records, previously described, is applied to the nominal structural model values and the resulting Cloud data pairs containing DCR_{LS} and the intensity measure $IM=S_a(T_1)$ are estimated for DS1, DS2, DS3, DS4, DS5. For reason of space, the results are shown only for DS3. Figure 5a represents the case in which the earthquake is applied on the gravity loads deformed structure (called Earthquake in Figure 5). Figure 5b, instead, represents the case in which the earthquake is applied on the gravity loads and settlements caused DS1 deformed structure (called DS1+Earthquake in Figure 5). Finally, Figure 5c represents the case in which the earthquake is applied on the gravity loads and settlements caused DS2 deformed structure (called DS2+Earthquake in Figure 5). The data pairs are plotted as yellow circles. The figures show in continue blue line the linear regression fitted in the logarithmic scale to the data. The Cloud Analysis-based model parameters are shown in Figure 5 (a, b and $\beta_{IM|DCR=1}$, see equations 1 and 2). The median IM at the onset of the damage state, $\eta_{IM|DCR=1}$ (i.e., the median of the fragility) can be obtained by finding the intensity value corresponding to unity from the regression line (as shown in Figure 5).

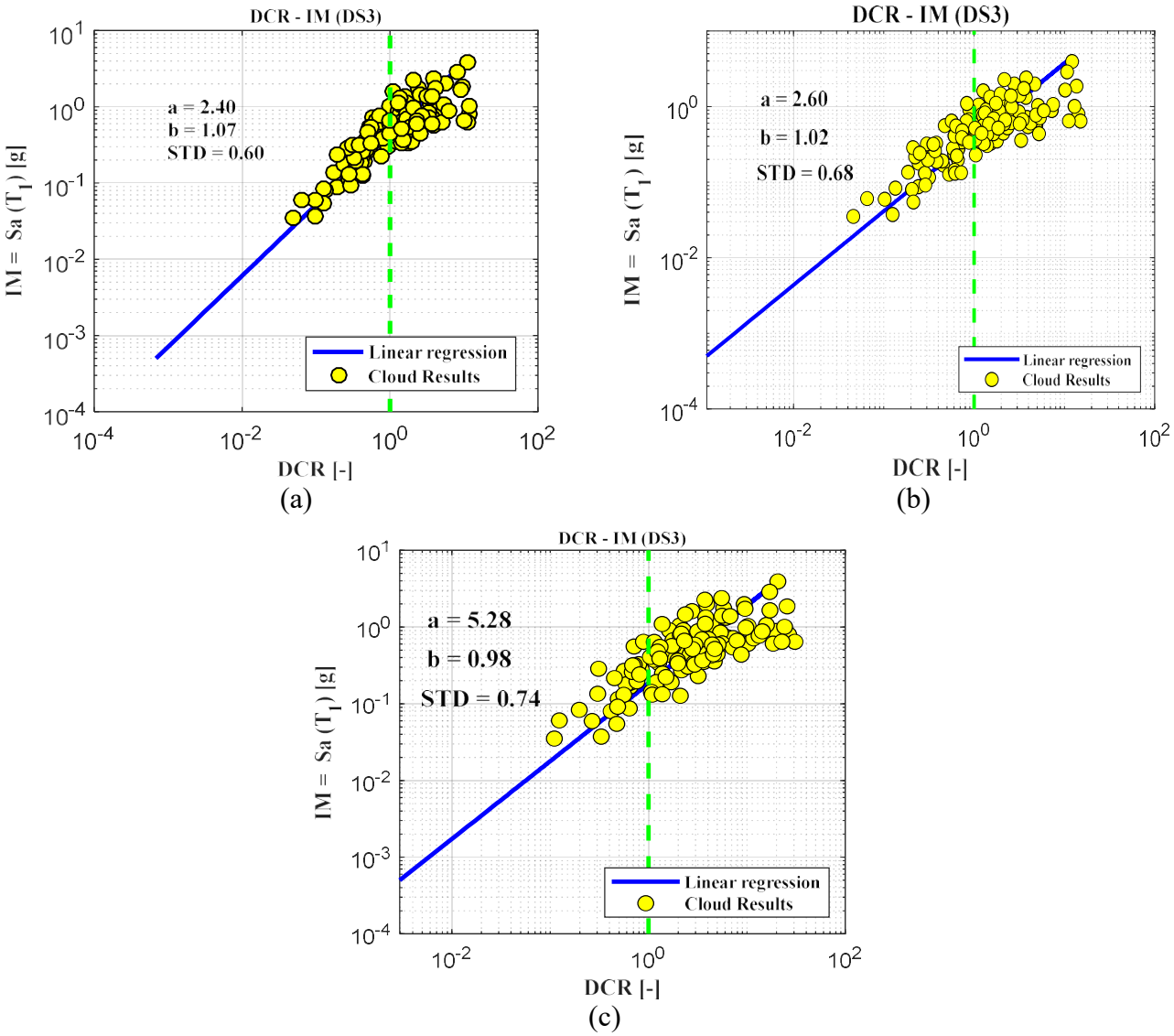

Figure 5: Cloud Analysis: (a) Earthquake, (b) DS1+Earthquake, (c) DS2+Earthquake.

Figure 6(a,b,c) show the Cloud Analysis-based fragility curves (based on Equation 3), obtained by employing the 150 records for the five damage states considered in this work. The Cloud Analysis-based Fragility curves are shown with the following colours: i) green for DS1; ii) yellow for DS2; iii) red for DS3; iv) blue for DS4; v) black for DS5. In Figure 6a, the curves are related to the case in which the earthquake is applied on the gravity loads deformed structure. Figure 6b, instead, represents the case in which the earthquake is applied on the gravity loads and settlements caused DS1 deformed structure (the relative fragility curves are added in the plot with dashed lines). Finally, Figure 6c represents the case in which the earthquake is applied on the gravity loads and settlements caused DS2 deformed structure (the relative fragility curves are added in the plot with dot-dashed lines).

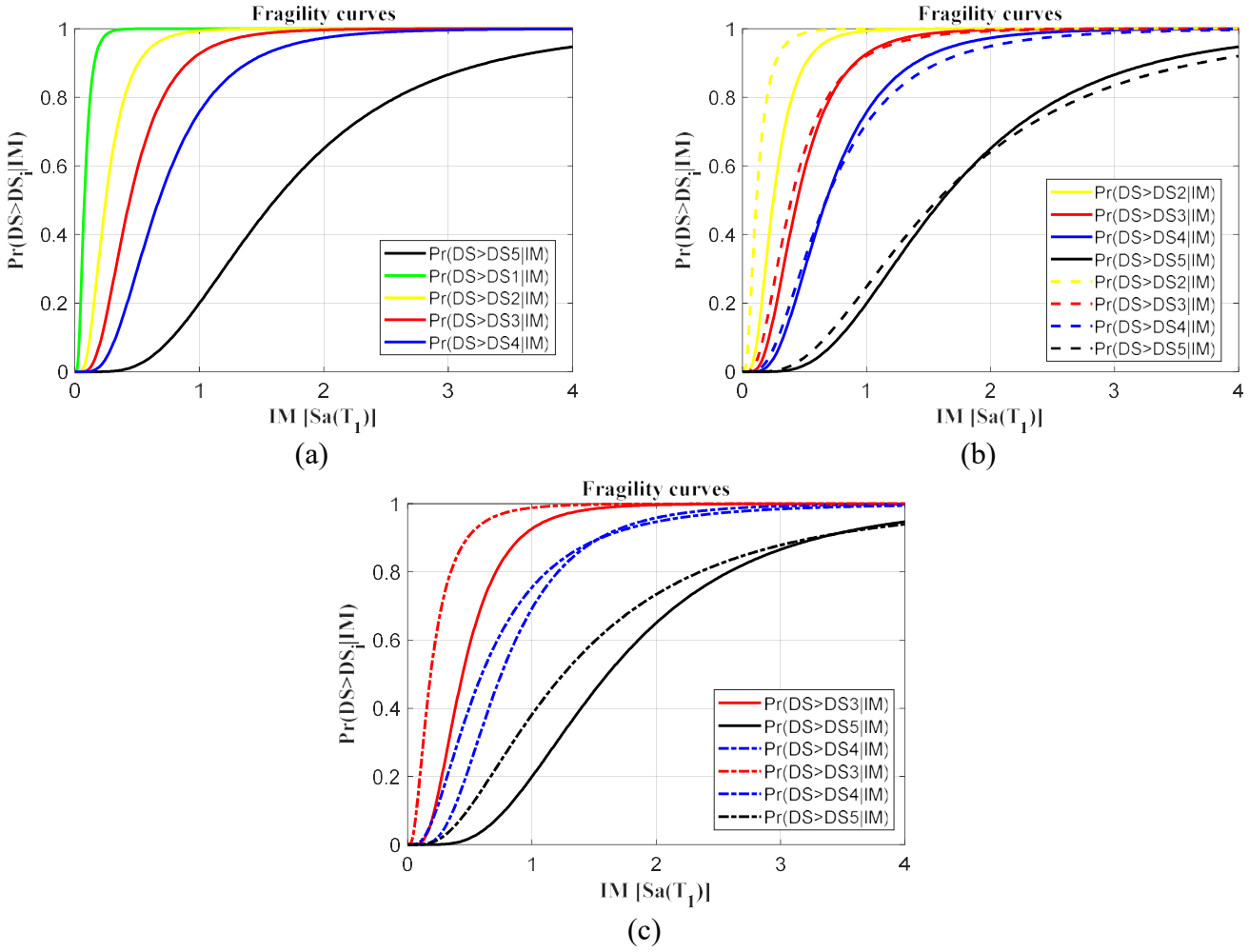

Figure 6: Fragility curves: (a) Earthquake, (b) DS1+Earthquake, (c) DS2+Earthquake.

4 CONCLUSIONS

The seismic assessment of reinforced concrete (RC) structures is commonly carried out neglecting potential previous damage induced by other phenomena, for example those related to the actions of slow-moving settlements. In this work, a typological 3D case study RC building, including also infills, is created according to gravity loads design. The seismic assessment of the building structural elements, caused by the design seismic action, is initially shown. Then, the seismic assessment is repeated, considering as point zero of the analysis the

"damaged" building as consequence of known slow-moving settlements. The non linear dynamic analysis known as Cloud is implemented herein on the equivalent SDOF system coming from the pushover analysis. Finally, an interesting comparison in terms of fragility curves is proposed between the safety condition of the building expected in both cases, with or without the consideration of the precedent induced displacements. The comparison of the results between the seismic assessment of the building expected in both cases, with or without the consideration of the precedent induced settlements, show the importance of this multi-hazard evaluation.

REFERENCES

[1] S. Bianchini, F. Pratesi, T.Nolesini, N. Casagli, Building deformation assessment by means of persistent scatterer interferometry analysis on a landslide affected area: The Volterra (Italy) case study. *Remote Sensing*, 7(4):4678-4701, 2015. https://doi.org/10.3390/rs70404678

[2] A. Miano, A. Mele, D. Calcaterra, D. Di Martire, D. Infante, A. Prota, M. Ramondini, The use of satellite data to support the structural health monitoring in areas affected by slow-moving landslides: a potential application to reinforced concrete buildings. *Struct Health Monit*, 20(6): 3265–3287, 2021. https://doi.org/10.1177/1475921720983232

[3] S. Arangio, F. Calò, M. Di Mauro, M. Bonano, M. Marsella, M. Manunta, An application of the SBAS-DInSAR technique for the assessment of structural damage in the city of Rome. *Structure and Infrastructure Engineering: Maintenance, Management, Life-Cycle Design and Performance*, 10(11):1469-1483, 2013. https://doi.org/10.1080/15732479.2013.833949

[4] D. A. Talledo, A. Miano, M. Bonano, F. Di Carlo, R. Lanari, ..., A. Stella, Satellite radar interferometry: Potential and limitations for structural assessment and monitoring. *J Build Eng*, 46. 103756, 2022. 10.1016/j.jobe.2021.103756

[5] A. Miano, F. Di Carlo, A. Mele, I. Giannetti, N. Nappo, M. Rompato, P. Striano, M. Bonano, F. Bozzano, R. Lanari, et al., GIS Integration of DInSAR Measurements, Geological Investigation and Historical Surveys for the Structural Monitoring of Buildings and Infrastructures: An Application to the Valco San Paolo Urban Area of Rome. *Infrastructures*, 7(89), 2022. https://doi.org/10.3390/infrastructures7070089

[6] Fotopoulou S, Karafagka S, Pitilakis K. Vulnerability assessment of low-code reinforced concrete frame buildings subjected to liquefaction-induced differential displacements. Soil Dyn Earthquake Eng 2018;110:173–84.

[7] Negulescu C, Foerster E. Parametric studies and quantitative assessment of the vulnerability of a RC frame building exposed to differential settlements. Nat Hazards Earth Syst Sci 2010; 10:1781–92.

[8] A. Miano, A. Mele, A. Prota, Fragility curves for different classes of existing RC buildings under ground differential settlements. Engineering Structures, 257, 114077, 2022.

[9] Mele A, Miano A, Di Martire D, Infante D, Ramondini M, Prota, A (2022) Potential of remote sensing data to support the seismic safety assessment of reinforced concrete buildings affected by slow-moving landslides. Arch Civ Mech Eng 22(2). 10.1007/s43452-022-00407-7

[10] T. Rossetto, A. Elnashai, Derivation of vulnerability functions for European-type RC structures based on observational data. *Eng Struct*, 25(10), 1241-1263, 2003.

[11] F. Jalayer, H. Ebrahimian, A. Miano, Intensity-based demand and capacity factor design: A visual format for safety checking. *Earthquake Spectra*, 36(4), 1952-1975, 2020.

[12] C. Del Gaudio, P. Ricci, G. M. Verderame, G. Manfredi G, Observed and predicted earthquake damage scenarios: the case study of Pettino (L'Aquila) after the 6th April 2009 event. *Bull Earthq Eng*, 14(10): 2643-2678, 2016.

[13] C. Del Gaudio, G. De Martino, M. Di Ludovico, G. Manfredi, A. Prota, P. Ricci, G. M. Verderame, Empirical fragility curves from damage data on RC buildings after the 2009 L'Aquila earthquake. *Bull Earthq Eng*, 15(4): 1425-1450, 2017.

[14] A. Miano, F. Jalayer, G. Forte, A. Santo, Empirical fragility assessment using conditional GMPE-based ground shaking fields: Application to damage data for 2016 Amatrice Earthquake. *Bulletin of Earthquake Engineering*, 18(15), 6629-6659. 2020.

[15] A. Singhal, A. S. Kiremidjian, Bayesian updating of fragilities with application to RC frames. *J Struct Eng* 124(8):922–929, 1998.

[16] P. Fajfar, A nonlinear analysis method for performance-based seismic design. *Earthquake spectra*, 16(3), 573-592, 200.

[17] NTC 2018 Commentary: Supplemento ordinario alla Gazzetta Ufficiale, n. 35 del 11 Febbraio 2019. Ministero delle Infrastrutture e dei Trasporti, Circolare 21 Gennaio 2019 "Istruzioni per applicare dell' «*Aggiornamento delle Norme tecniche per le costruzioni» di cui al decreto ministeriale 17 Gennaio 2018*".

[18] F. Jalayer, R. De Risi, G. Manfredi, Bayesian Cloud Analysis: efficient structural fragility assessment using linear regression. Bulletin of Earthquake Engineering, 13(4), 1183-1203, 2015.

[19] F. Jalayer, H. Ebrahimian, A. Miano, G. Manfredi, H. Sezen, Analytical fragility assessment using unscaled ground motion records. *Earthquake Engineering & Structural Dynamics*, 46(15), 2639-2663, 2017.

[20] F. Jalayer, H. Ebrahimian, A. Miano. Record-to-record variability and code-compatible seismic safety-checking with limited number of records. Bulletin of Earthquake Engineering, 19(15), 6361-6396, 2021.

[21] F. Jalayer, H. Ebrahimian, A. Miano, A. N2 with Cloud: A Non-Linear Dynamic Analysis Procedure for the Equivalent SDOF System. *XVIII Convegno ANIDIS L'ingegneria Sismica in Italia*, Ascoli Piceno, 15-19 settembre, 2019, ID: 4548155. DOI: 10.1400/271224.

[22] Grünthal G. Cahiers du centre européen de géodynamique et de séismologie: volume 15 – european macroseismic scale1998. Luxembourg: European Center for Geodynamics and Seismology; 1998.

[23] D. Cardone, G. Perrone, Developing fragility curves and loss functions for masonry infill walls. *Earthquak Struct*, 9(1): 257–279, 2015.

[24] C. Del Gaudio, M. T. De Risi, P. Ricci, G. M. Verderame, Empirical drift-fragility functions and loss estimation for infills in reinforced concrete frames under seismic loading. *Bulletin of Earthquake Engineering*, 17, 1285-1330, 2019.

[25] C. Del Gaudio, P. Ricci, G. M. Verderame, G. Manfredi, Urban-scale seismic fragility assessment of RC buildings subjected to L'Aquila earthquake. *Soil Dynamics and Earthquake Engineering*, 96, 49-63, 2017.

[26] C. Del Gaudio, P. Ricci, G. M. Verderame, A class-oriented mechanical approach for seismic damage assessment of RC buildings subjected to the 2009 L'Aquila earthquake. *Bulletin of Earthquake Engineering*, 16, 4581-4605, 2018.

[27] H. Aslani, E. Miranda E, Probabilistic earthquake loss estimation and loss disaggregation in buildings. Diss Stanford University; 2005.

[28] M. Di Domenico, M. T. De Risi, V. Manfredi, M. Terrenzi, G. Camata, F. Mollaioli, ... & G. M. Verderame, Modelling and seismic response analysis of Italian pre-code and low-code reinforced concrete buildings. Part II: infilled frames. *Journal of Earthquake Engineering*, 1-31, 2022.

[29] M. T. De Risi, M. Di Domenico, V. Manfredi, M. Terrenzi, G. Camata, F. Mollaioli, ... & G. M. Verderame, Modelling and seismic response analysis of Italian pre-code and low-code reinforced concrete buildings. Part I: Bare frames. *Journal of Earthquake Engineering*, 1-32, 2022.

[30] G. M. Verderame, M. Polese, C. Mariniello, G. Manfredi, A simulated design procedure for the assessment of seismic capacity of existing reinforced concrete buildings. *Advances in Engineering Software*, 41(2), 323-335, 2010.

[31] G. Al-Chaar, Evaluating Strength and Stiffness of Unreinforced Masonry Infill Structures. Report, ERDC/CERL TR-02-1, January 2002.

[32] M. N. Fardis, Seismic Design, Assessment and Retrofitting of Concrete Buildings: based on EN-Eurocode 8. Springer Verlag, 2009.

[33] D. Biskinis, M. N. Fardis, Deformations at flexural yielding of members with continuous or lap-spliced bars. *Struct Concr*, 11(3):128–38, 2010a.

[34] D. Biskinis, M. N. Fardis, Flexure-controlled ultimate deformations of members with continuous or lap-spliced bars. *Struct Concr*,11(2):93–108, 2010b.

[35] T. B. Panagiotakos, M. N. Fardis MN, Seismic response of infilled RC frames structures. In: 11th World Conference on Earthquake Engineering, Acapulco, México, June 23–28, 1996 [Paper No. 225].

[36] DM 17/01/18 (2018) Norme tecniche per le costruzioni, Ministerial Decree. (in italian)

[37] C. Smerzini, C. Galasso, I. Iervolino, R. Paolucci, Ground motion record selection based on broadband spectral compatibility, *Earthq Spectra*, 30, 1427–1448, 2014.

[38] T. Rossetto, P. Gehl, S. Minas, C. Galasso, P. Duffour, J. Douglas, O. Cook, FRACAS: A capacity spectrum approach for seismic fragility assessment including record-to-record variability, *Eng Struct*, 125, 337–348, 2016.

[39] R. Gentile, C. Galasso, Y. Idris, I. Rusydy, E. Meilianda, From rapid visual survey to multi-hazard risk prioritisation and numerical fragility of school buildings. *Natural Hazards and Earth System Sciences*, 19(7), 1365-1386, 2019.